

Monika Grasser^a, Andreas Ludwig^a, Wolfram Schillinger^b

^aUniversity of Leoben, Department of Metallurgy, Christian-Doppler Laboratory for Multiphase Simulation of Metallurgical Processes, Chair of Simulation and Modelling of Metallurgical Processes, Leoben, Austria

^bWieland-Werke AG, Central Laboratory, Research & Development, Ulm, Germany

Thermodynamic description of the system Cu–Sn–P experimental and numerical investigation

The aim of the presented experimental and numerical investigation is to verify the ternary phase diagram Cu–Sn–P in the Cu-rich corner, especially the presence and position of the ternary eutectic transition point. Annealing experiments within a concentration gradient have been performed and compared to computational thermodynamics. The identification of phases and phase regions is based on differential thermal analysis, and scanning electron and light microscopy. The discussed ternary eutectic transition in the Cu-rich corner is confirmed, phases and phase regions, as proposed by computational thermodynamics, are verified. In addition, the existence of the γ phase could be confirmed but the ε phase was not found in the as-cast microstructures which decreases its importance for technical bronze alloys with Sn up to a mass fraction of 0.2.

Keywords: Thermodynamics; Cu–Sn–P; Ternary; Phase diagram

1. Introduction

Commercial bronze alloys exhibit a tin (Sn) content in the range of 0.04–0.13 mass fraction and a phosphorus (P) content of up to 0.01 mass fraction. For this reason the copper (Cu)-rich corner of the ternary system Cu–Sn–P is of particular interest. In spite of numerous studies on the ternary system Cu–Sn–P (e.g. Refs. [1–7]), there are still open questions about the existence of a ternary eutectic point and about the occurrence of the phases γ and ε [5]. The existence of a ternary eutectic point at a mass fraction of Sn of 0.148 and of P of 0.045 was proposed in several publications from 1910 to 1937 [8–11]. Other authors (e.g. [1, 12]) suggested that this “ternary eutectic” should rather be a transition reaction $L + \alpha \rightarrow \beta + \text{Cu}_3\text{P}$ (where L is the liquid and α , β and Cu_3P the appearing phases). This was also concluded in a more recent experimental differential thermal analysis (DTA) study on the ternary system [7] where, in addition, the occurrence of the γ phase was not observed.

Due to the significant advances in computer technology during recent years, a new attempt to answering these open questions can be taken by connecting experimental investigations and thermodynamic calculations using the CALPHAD approach. The CALPHAD approach was developed during the last decades for a comprehensive combination of

thermodynamic and kinetic models. It has evolved from performing complex equilibrium calculations relevant to materials science to simulate phase transformations involving diffusion. Although the simulation of thermodynamic properties is based on experimental observations, the computational power helps to decide where particular experiments have to be performed in order to validate and improve already established thermodynamic information. This allows the prediction of material composition, structures and properties resulting from various processing steps.

Since 1997, the Ringberg Workshops on Computational Thermodynamics have produced two reports on the status and evolution of “Applications of Computational Thermodynamics” [13, 14]. Various publications on applications of computational thermodynamics are given in Refs. [15–20].

The present publication places emphasis on computational thermodynamic investigations of the ternary Cu–Sn–P system in the Cu-rich corner using the thermodynamic software Thermo-Calc and on experimental investigations to validate this data. Details about Differential Scanning Calorimetry (DSC) measurements and annealing experiments on the two binary systems Cu–Sn and Cu–P can be found in a previous publication [21]. In the following at first the thermodynamic description of the system Cu–Sn–P is given to catch up with the results presented by Miettinen 2001 [6]. After that details are given to experimental observations on annealing experiments followed by a discussion for both, the computational and experimental investigation.

2. Thermodynamic description of the system

The here presented isothermal sections and isopleths are performed using the numerical Cu–Sn–P database CuSnII [22] which is based mainly on [6] and was implemented by Thermo-Calc in 2005 for this work. Miettinen [6] presented a description of the ternary system in 2001 comparing his assessment work with experimental investigations performed by [7]. Numerous calculations have been performed during the recent study to achieve a detailed numerical description of the ternary system Cu–Sn–P in the Cu-rich corner in the range of up to a mass fraction of 0.15 P and 0.35 Sn. Due to the limited range of the assessed database, information outside this range is not displayed. The presented isothermal sections are shown to describe the ternary system in detail.

Isothermal sections for $T = 1305, 1173, 1053, 973, 918, 913, 798,$ and 573 K are given in Fig. 1. In addition, a three-dimensional (3D) projection of the liquidus surface of the ternary phase diagram is shown. The front view displays the binary section Cu–Sn with a mass fraction of 0 to 0.35 Sn. At $T = 1305$ K, which is below the melting point of pure Copper ($T_{1,Cu} = 1358$ K), there are two single-phase regions α and L which are separated by a two-phase region $\alpha + L$ as expected according to the Gibbs phase rule. The compound Cu_3P has a melting temperature of $T_{1,Cu_3P} = 1295$ K. Therefore, in the isothermal section at $T = 1173$ K this compound appears as a point which is surrounded by a two-phase region $Cu_3P + L$. The peritectic transition $L + \alpha \rightarrow \beta$ occurs at temperatures below $T = 1072$ K, thus in the isothermal section at $T = 1053$ K β is present and the first three-phase region $\alpha + \beta + L$ (triangle, Fig. 1, $T = 1053$ K) is observed. During further cooling, another peritectic transition

$L + \beta \rightarrow \gamma$ takes place at $T = 1028$ K. In the isothermal section at $T = 973$ K, the γ phase is present and the three-phase region $\beta-\gamma-L$ is cut appearing in a triangular shape. Besides, the eutectic groove between α and Cu_3P is reached and the three-phase region $\alpha-Cu_3P-L$ is visible (Fig. 1, $T = 973$ K). Further cooling leads to a decrease of the L region to a small area in the isothermal section at $T = 918$ K. At a slightly lower temperature, namely at approximately $T_E = 917$ K, the ternary eutectic point is reached at a mass fraction of 0.15 Sn and 0.55 P (T_E , Fig. 1) where the eutectic reaction of $L \rightarrow \alpha + \beta + Cu_3P$ is proposed. Here the assessment work of [7] differs from the interpretation of [5] who rather proposes a transition reaction of $L + \alpha \rightarrow \beta + Cu_3P$ at ~ 928 K based on experimental work of [1, 7, 12].

At $T = 918$ K the decrease of the liquid phase leads to the presence of two additional three-phase regions, namely $Cu_3P-\gamma-L$ and $Cu_3P-\varepsilon-\gamma$. Further cooling of a few degrees

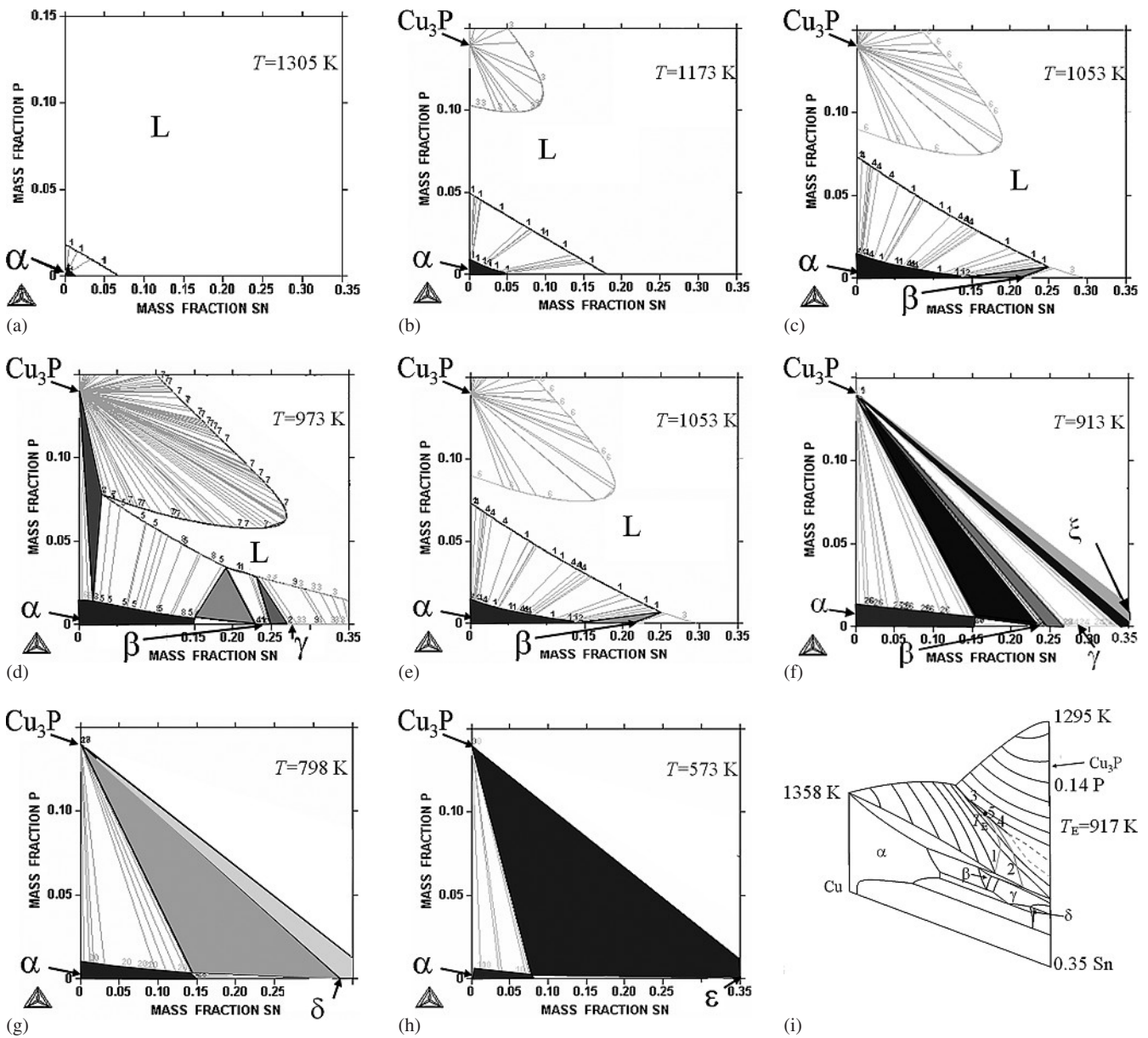


Fig. 1. The isothermal sections of the ternary phase diagram of Cu–Sn–P in the Cu-rich corner calculated with ThermoCalc (database CuSnII [22]) are shown for (a) $T = 1305$, (b) $T = 1173$, (c) $T = 1053$, (d) $T = 973$, (e) $T = 918$, (f) $T = 913$, (g) $T = 798$, and (h) $T = 573$ K. In addition, (i) shows a 3D projection of the liquidus surface of the ternary phase diagram. α = Cu (max. Sn 0.158 mass fraction, P 0.02 mass fraction); β $\sim Cu_{17}Sn_3$; γ $\sim Cu_3Sn$; δ $\sim Cu_{41}Sn_{11}$; ε $\sim Cu_3Sn$; ξ $\sim Cu_{10}Sn_3$ (nomenclature taken from [5]). The 3D liquidus surface is displayed up to 0.35 mass fraction Sn and 0.14 mass fraction P.

leads to the presence of the ξ phase (ξ) within the three phase region Cu_3P - γ - ξ . The ε phase (ε) has a concentration of ~ 0.38 mass fraction Sn and ξ of ~ 0.36 mass fraction Sn. These two phases are not expected to resolve any P. At $T = 913$ K four three-phase regions are present, namely Cu_3P - ε - ξ , Cu_3P - γ - ξ , Cu_3P - β - γ , and Cu_3P - α - β (Fig. 1, $T = 913$ K). Note that the two-phase region Cu_3P - ε which separates the two three-phase regions Cu_3P - γ - ξ and Cu_3P - ε - ξ is narrow and cannot be seen in Fig. 1f. At $T = 798$ K the δ phase (δ) is stable while ξ disappeared caused by the peritectoid reaction $\xi + \gamma \rightarrow \delta$. In this section the three-phase regions of Cu_3P - δ - ε and Cu_3P - α - δ are present. β disappeared due to the eutectoid reaction $\beta \rightarrow \alpha + \gamma + \text{Cu}_3\text{P}$ below $T = 861$ K. With further cooling only the solubility of Sn in α is decreasing till ~ 623 K is reached. Here, the last transition reaction, namely the eutectoid reaction $\delta \rightarrow \alpha + \varepsilon + \text{Cu}_3\text{P}$ is expected. In the last picture of Fig. 1i the liquidus surface of the Cu-rich corner is redrawn based on calculations performed with Thermo-Calc and shown in Fig. 1a – h. Here, the black lines define the isotherms and the numbered lines the mono variant lines (1) for the peritectic reaction $L + \alpha \rightarrow \beta$, (2) for the peritectic reaction $L + \beta \rightarrow \gamma$, and (3) for the eutectic reaction $L \rightarrow \text{Cu}_3\text{P} + \alpha + L$ which ends in the ternary eutectic point (T_E). (4) represents the monovariant line of the eutectic reaction $L \rightarrow \text{Cu}_3\text{P} + \gamma + L$ and attached to it (5) shows the one of the eutectic reaction $L \rightarrow \text{Cu}_3\text{P} + \beta + L$ which also ends in the ternary eutectic point (T_E).

3. Experimental procedure

In this section findings gained by annealing experiments will be described. The performance of the annealing experiments was described in detail in the work of [23, 24]. A cylindrical geometry is used consisting of a Cu casing (about 0.002 m extension and a radius of about 0.008 m) and a core of Cu–Sn–P [23, 24]. In addition, the sample is closed at the top and the bottom by Cu pieces to avoid evaporation of P. After annealing, the samples were quenched in cold water and prepared for scanning electron microscopy (SEM), light microscopy (LM), and microprobe investigations. The temperature range and sample concentrations for the experimental study were chosen on the one hand to prove already published data and on the other hand to gain more information about the ternary eutectic point of the Cu-rich corner of this system. The studies on the binary system, including DSC measurements and annealing work, are published in [21]. Here, a summary of the performed investigations on the ternary system is given. The identification of the different phases is based on SEM and LM in combination with published phase diagram data. Here, three distinct annealing experiments are discussed which have been performed

- (i) at 921 K for 6 days,
- (ii) at 917 K for 20 days, and
- (iii) at 915 K for 20 days

with a measured average deviation of the temperature during annealing of $\Delta T_a = \pm 1$ K. The measurement accuracy for the detection of Sn and P is $\Delta c^{P,Sn} \sim \pm 0.005$ mass fraction. After annealing, the samples were quenched in cold water and prepared for further investigations.

4. Results and discussion

In this section a comparison of the description of the ternary system Cu–Sn–P in the Cu-rich corner to literature is given

and discussed. As a further step the calculated phase diagram information is verified by the experimental measurements.

4.1. Computational thermodynamics

The aim of the study concerning the computational thermodynamics was to show that the used database enables an accurate description of the thermodynamics of the system Cu–Sn–P in the Cu-rich corner in comparison to literature. At first it has to be mentioned, that database CuSnII handles the phases δ , ε , and ξ as compounds which is a simplification of the phase diagram published and discussed by [25]. Besides, the calculations performed with Thermo-Calc show good agreement with the phase diagram proposed by [21]. Although the γ phase was not detected in the experimental work performed by [7], [6] included the γ phase in the assessment work for the ternary phase diagram. γ is thought to form out of β during cooling, whereas both phases are thought to have fcc structure. Further cooling leads to eutectoid decomposition of γ at 793 K to α and δ [26]. According to Schuhmann, neither β nor γ can be observed after quenching at room temperature, here metastable transition states are observed that sometimes show martensitic structure [26].

Calculations with Thermo-Calc (database CuSnII) propose the ternary eutectic point at $T_E = 917$ K (see Fig. 1). According to [5] the ternary eutectic reaction is still questionable and instead a transition of $L + \alpha \rightarrow \beta + \text{Cu}_3\text{P}$ is suggested within a range from 915 K to 928 K. That is why we investigated especially this area in the phase diagram.

4.2. Annealing experiments

Figure 2 displays a micrograph of the unannealed ternary sample with the Cu casing and the ternary inner cylinder out of CuSn20P6 (nominal concentration). It can be seen that a small gap is present between the two sample partners. In addition, the CuSn20P6 core shows porosity which is caused by the rigidity of this ternary alloy. A fine-structured matrix within areas of Cu_3P (Fig. 2b) is visible in the SEM picture of a region with higher magnification as marked by the rec-

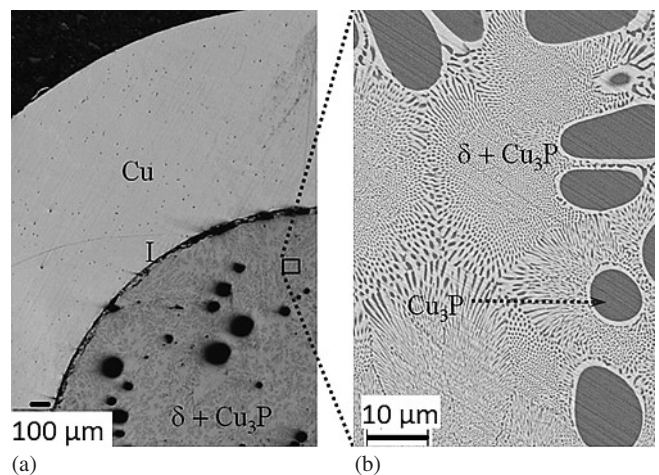


Fig. 2. (a) Micrograph of a reference sample consisting of Cu casing and CuSn20P6 core. “I” marks the position of the interface between the two sample materials; (b) SEM picture shows (black square indicated in the left picture) δ and Cu_3P eutectic/eutectoid around Cu_3P areas.

tangle in Fig. 2a. It can be seen that the matrix around the Cu_3P areas has eutectic/eutectoid microstructure containing $\delta\text{-Cu}_3\text{P}$ eutectic/eutectoid. The detected average concentrations for the different phases are listed in Table 1. All measurements have been performed by EDS and/or WDS.

Figure 3a shows a SEM picture of a cross-section of the sample after annealing at 921 K and Fig. 3b a corresponding magnification of a certain area. The interface between the two sample partners is thought to be at the position of the pores marked with “I” (Fig. 3a). It has to be mentioned that the pores observed in the core of the reference sample are not visible anymore. The pores and cracks in Fig. 3 are thought to be formed after quenching due to solidification shrinkage.

Visually, it is possible to distinguish four different regions in Fig. 3.

- (i) is the one-phase region of the outer Cu ring (middle gray) which has increasing Sn and P content in the region close to the interface between the samples (marked with “I”) and
- (ii) is the two-phase region attached. (iii) and (iv) mark a slightly darker region with a relatively homogeneous matrix.
- (iii) appears attached to the two-phase region in the lower part of the picture and
- (iv) in the centre of the sample. Attached to the big Cu_3P area (marked “II” in Fig. 3, a small two-phase region with eutectic growth is visible close to a fine-structured region that is slightly brighter than the surrounding areas.

Measurements indicate that this two-phase region and the region marked with (ii) consist of $\alpha + \text{Cu}_3\text{P}$. The detected average concentrations for the different phases are listed in

Table 1. Detected average concentrations for the different phases observed in the reference sample before annealing (mass fraction of 0.2 Sn and 0.06 P) given in mass fraction.

Phase region	Sn	P
Cu_3P		0.146
δ	0.316	
$\text{Cu}_3\text{P} + \delta$	0.283	0.38

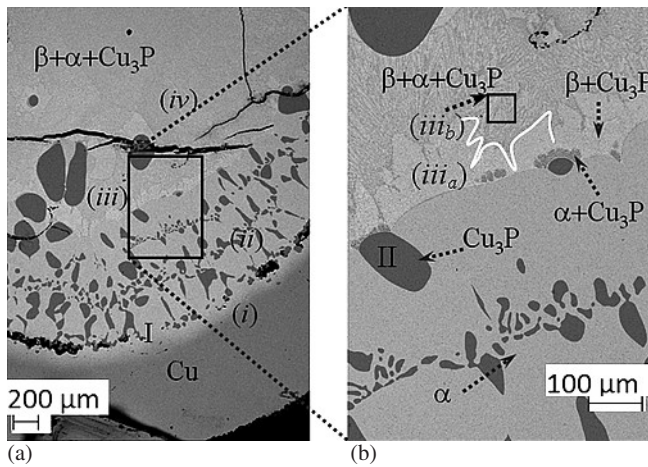


Fig. 3. (a) SEM picture of the annealing sample (mass fraction of 0.2 Sn and 0.06 P) at 921 K for 6 days; (b) the black square (indicated in the left picture) is displayed with higher magnification. Sn diffusion is observed up to $\sim 150 \mu\text{m}$ into the outer Cu tube. Further details are given in the text.

Table 2. Detected average concentrations for the different phases observed in the sample annealed at 921 K for 6 days after quenching (mass fraction of 0.2 Sn and 0.06 P) given in mass fraction.

Phase region	Sn	P
Cu_3P		0.132
α	1.25	0.20
β	0.235	0.05
$\text{Cu}_3\text{P} + \alpha$	0.107	0.46
$\text{Cu}_3\text{P} + \beta$	0.17	0.47
$\text{Cu}_3\text{P} + \alpha + \beta$ (iii _b)	0.147	0.46

Table 2. In Fig. 3 it can also be seen that there is a second two-phase region observed in region (iii), $\beta + \text{Cu}_3\text{P}$. Besides, there is a three-phase region identified containing $\alpha + \beta + \text{Cu}_3\text{P}$ (iii_b). These three phases are observed three times with different phase fractions and, with that in areas of different average concentrations. Figure 4 shows SEM pictures of these three areas.

Figure 5a shows a micrograph of the sample annealed at 917 K for 20 days. The small gap appearing at the interface between the ternary sample (inner cylinder) and the Cu casing seems to collect Cu_3P and is therefore enriched in P (up to 0.07 mass fraction P) but depleted in Sn (~ 0.06 mass fraction Sn). Attached to the interface a two-phase region of $\alpha\text{-Cu}_3\text{P}$ is observed due to the loss of tin into the Cu casing. The boundary between the two-phase region and the attached three-phase region is not very clear defined. Although the microstructure in the centre of the sample seems to consist of two phases, the SEM picture after etching illustrates the complex microstructure of the sample (see Fig. 9a in the discussion). Here, it has to be kept in mind that the gray scale difference as well as the structure of the different phases is strengthened by etching. Figure 5b shows the marked region in Fig. 5a with a higher magnification. Here, the transition from the two-phase region $\alpha\text{-Cu}_3\text{P}$ at the boundary to the three-phase region $\beta\gamma\text{-Cu}_3\text{P}$ in the centre of the sample. The detected concentrations of the appearing phases confirm the previous measurements.

However, since the γ phase appears as a very fine microstructure after etching (see Fig. 9) it is not possible to identify it clearly by SEM. Figure 6a shows a micrograph of the sample annealed at 915 K and 20 days. Figure 6b displays a similar area as indicated by the dark square at a higher magnification and allows a closer look at the microstructure. Here, a similar structure is observed as in the latter sample. Again, the microstructure in the centre of the sample seems to consist of two phases, but the SEM picture after etching illustrates that there is a third phase appearing. Attached to the Cu_3P area, visible on the left hand side of Fig. 6b, a region with a needle-like structure (probably γ) is observed. The slightly darker region has a more or less uniform matrix. It has a slightly lower Sn concentration than the surrounding regions and no remarkable P content (β).

Based on the fact, that, due to annealing homogenization of the sample takes place, the phase distribution of the reference sample is not discussed here. It appears that the actually observed phase distribution of the annealing sample at 921 K is caused by a phase transition sequence during the 6 days of annealing as described in the following and schematically drawn in Fig. 7. The outer Cu tube has a melting

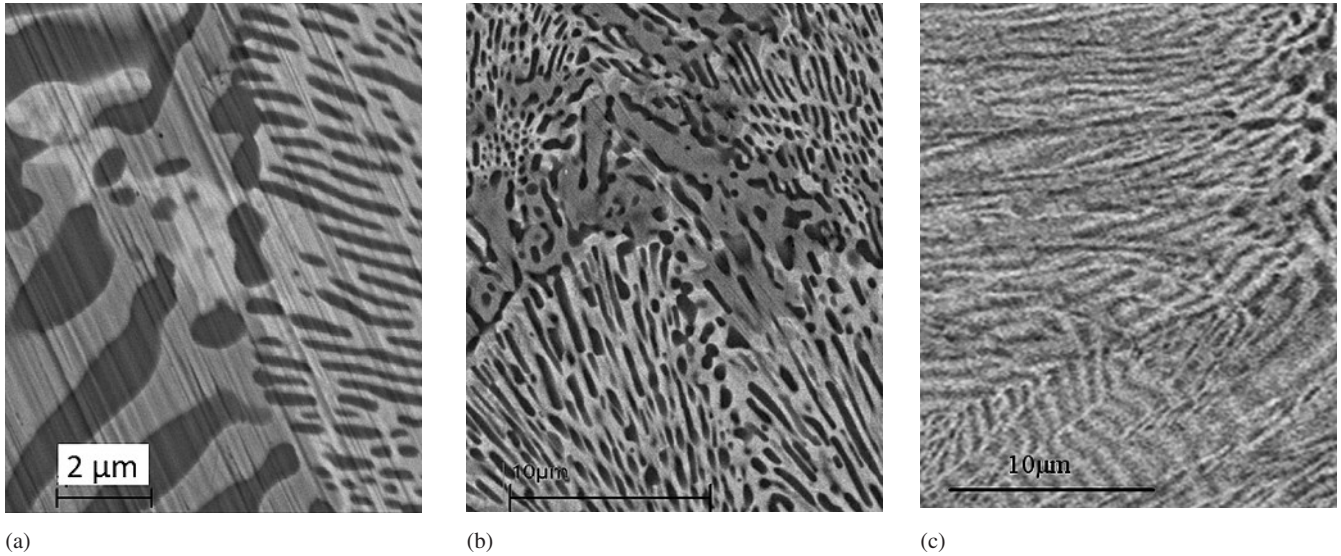


Fig. 4. Three-phase regions observed after annealing at 921 K and quenching. Occurring phases: α (middle gray), β (bright gray), Cu_3P (dark gray). (a) shows a small three-phase region between the two two-phase regions, $\text{Cu}_3\text{P} + \alpha$ and $\text{Cu}_3\text{P} + \beta$ attached to a Cu_3P "grain" as shown in Fig. 3 (labelled with "II"). (b) shows the three-phase region (iii_b) attached to the two-phase region $\text{Cu}_3\text{P} + \beta$ (iii_a) indicated in Fig. 3 (right), and (c) the three-phase region in the centre of the sample, indicated by (iv) in Fig. 3 (right).

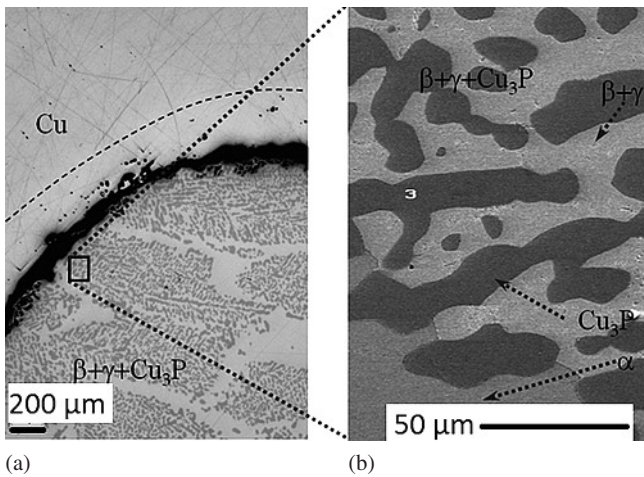


Fig. 5. Annealing sample consisting of Cu casing and CuSn20P6 (mass fraction of 0.2 Sn and 0.06 P) core. (a) Micrograph of the sample annealed at 917 K for 20 days; (b) higher magnification of an area close to the depletion zone indicated by the black square. Sn diffusion is observed up to about $\sim 350 \mu\text{m}$ into the outer Cu tube indicated by the broken line whereas no remarkable P content is detected ahead of the boundary between the samples. White number indicates the position of SEM measurements.

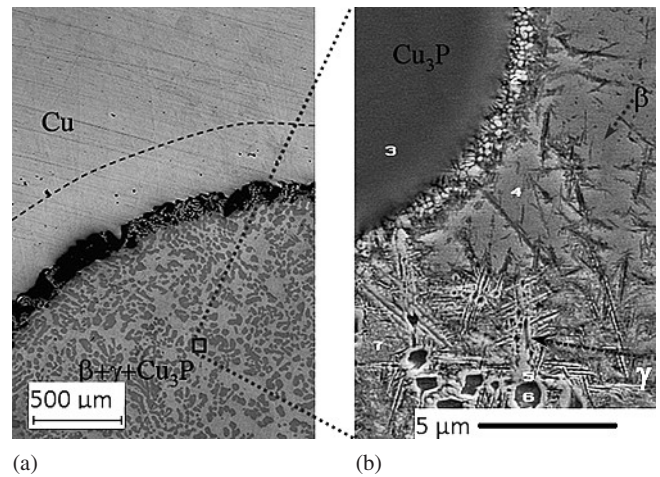


Fig. 6. Annealing sample consisting of Cu casing and CuSn20P6 (mass fraction of 0.2 Sn and 0.06 P) core. (a) Micrograph of the sample annealed at 915 K for 20 days, (b) higher magnification of a similar area as indicated by the black square. Sn diffusion is observed up to about $\sim 350 \mu\text{m}$ into the outer Cu tube indicated by the broken line whereas no remarkable P content is detected ahead of the boundary between the samples. White numbers indicate the position of SEM measurements.

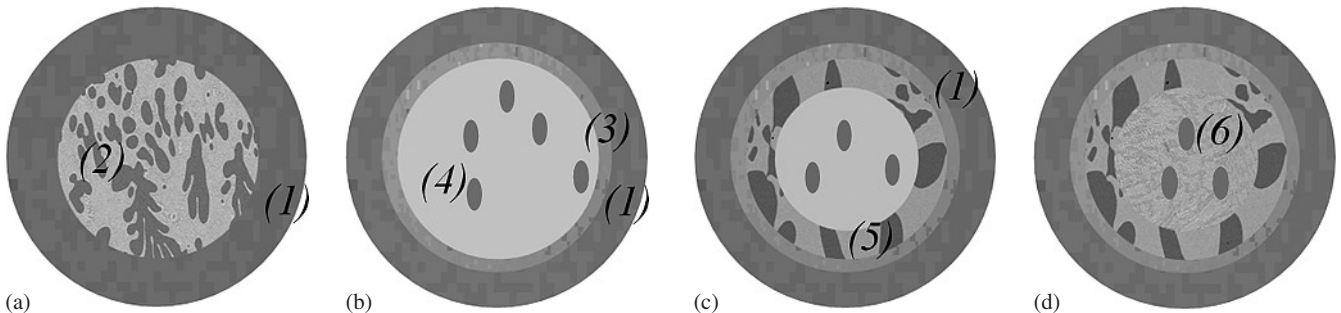


Fig. 7. Schematic drawing of the diffusion and melting/solidification sequence of the annealed sample. (a) displays the sample before annealing (1) Cu casing, (2) CuSn20P6 (mass fraction of 0.2 Sn and 0.06 P); (b) The solid Cu shell shows diffusion of Sn and P (3). At 921 K a two-phase region is expected in the inner cylinder CuSn20P6 (mass fraction of 0.2 Sn and 0.06 P) (4), where Cu_3P and liquid L are in equilibrium. (c) shows that α and Cu_3P grow as soon as the necessary concentration for the two-phase region of thermodynamic equilibrium is reached (5). In the centre the liquid is depleted in P and enriched in Sn, but still liquid. (d) Quenching leads to rapid solidification of the liquid and ternary eutectic (α , β , Cu_3P) is formed (6).

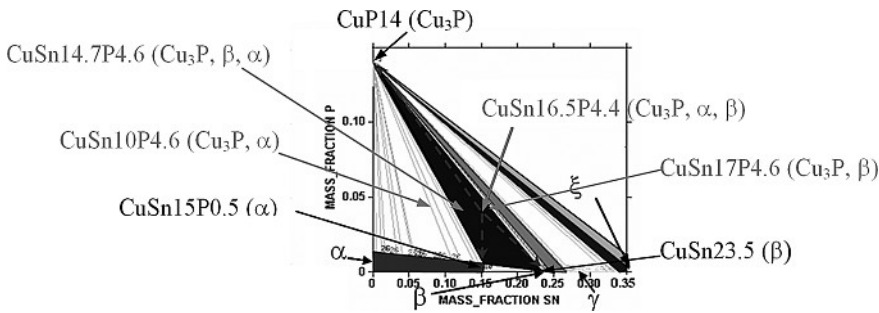


Fig. 8. Isothermal section of the Cu–Sn–P system in the Cu-rich corner at 913 K. It is visible that the P content is about the same in all of the two- or three-phase regions, whereas the Sn content varies significantly.

temperature of 1358 K and is therefore expected to stay solid during annealing (Fig. 7a (1)). The ternary alloy CuSn20P6 of the inner cylinder (Fig. 7a (2)) initially consists of a matrix of δ Cu₃P and Cu₃P areas. Here, it has to be mentioned that the ϵ phase, which is proposed by equilibrium thermodynamics was not found in any sample at lower temperature as proposed by literature [6, 7]. At the applied annealing temperature the two-phase region Cu₃P and liquid (Fig. 7b (3)) is the equilibrium phase distribution according to the thermodynamic phase diagram. Based on the melting temperature of Cu₃P, the Cu₃P areas are not expected to melt during annealing. Sn and P are expected to diffuse from the ternary sample into the Cu tube (Fig. 7b (1)) enriching this area of α (Fig. 7b (4)). Here, it has to be mentioned, that P tends to diffuse about 10 times slower than Sn [21]. The diffusion behaviour leads to an increase of the liquidus temperature in the inner sample close to the solid–liquid interface and therefore α is expected to grow. As the concentration of the two-phase region is reached, Cu₃P is in equilibrium with α and the two-phase region is developing (Fig. 7c (5)). Due to quenching, solidification starts very rapidly which leads to fine imbedding of Cu₃P at the grain boundaries of α at the solid and liquid interface. Figure 3 shows two Cu₃P areas which are surrounded by a two-phase eutectic region. In addition, a three-phase region with not clearly defined boundaries is occurring close to it and, attached, a second two-phase region with eutectic structure of Cu₃P + β is observed (Fig. 3). These examples indicate that the liquid solidifies rapidly due to quenching, as expected, and therefore the thermodynamic equilibrium is not reached in some regions. Hence, the three-phase region observed (Fig. 7d (6)) in the centre of the sample shows a rather fine microstructure which indicates that Cu₃P + β + α have been formed out of the liquid during quenching. This phase distribution, observed after annealing at 921 K and quenching, indicates that the phase transition as proposed by [6] $L + \alpha \rightarrow \beta + \text{Cu}_3\text{P}$ should be rather a eutectic transition of $L \rightarrow \alpha + \beta + \text{Cu}_3\text{P}$.

Figure 8 gives a comparison of the detected concentrations with computational thermodynamics at 913 K, just slightly below the expected ternary eutectic point. The detected concentrations and phase distributions are marked for the different phase regions of the annealed sample after quenching. The P content of β in this case is high in comparison to published data, where almost no P is expected. Since the regions containing β show a very fine phase distribution ($\sim 1 \mu\text{m}$) the detected concentrations are not reliable. The overall P content in the two- and three-phase regions lies around 0.045 mass fraction P whereas the Sn content varies between 0.10 to 0.17 mass fraction Sn. The measured concentration in the centre of the sample is indi-

cated by the broken arrows. The expected concentrations of the phases at the ternary eutectic point are, according to the phase diagram information, 0.15 mass fraction Sn and 0.006 mass fraction P for α , 0.14 mass fraction P for Cu₃P, and 0.235 mass fraction Sn for β . The measured concentrations as shown in Fig. 8 are, concerning the uncertainties of the detection of Sn and P with EDS/WDS of $\Delta c^{\text{P,Sn}} \sim \pm 0.005$ mass fraction, in good agreement with the assessed data used in the database CuSnII. The three-phase region observed in the centre of the sample indicates that the phase transition as proposed by [5] $L + \alpha \rightarrow \beta + \text{Cu}_3\text{P}$ should rather be an eutectic transition of $L \rightarrow \alpha + \beta + \text{Cu}_3\text{P}$ at approximately CuSn15P5.

The next two discussed samples are annealed at lower temperatures, as shown in Fig. 5 and Fig. 6, namely at 917 K (Fig. 9a) and 915 K (Fig. 9b) for 20 days. A schematic phase distribution of the two samples and an SEM picture after etching of each sample is displayed in Fig. 9. Here (1) indicates the pure Cu tube, (2) marks the area where after annealing diffusion of Sn into the Cu tube is observed. (3) marks the small Sn depleted area in the CuSn20P6 cylinder where in both samples a two-phase region of α -Cu₃P is observed, whereas (4) indicates the three-phase regions in the centre. The broken line indicates the porous, P-rich boundary between the annealing partners.

According to the phase diagram, the samples are situated at or just above of the eutectic plane. Thermodynamics pro-

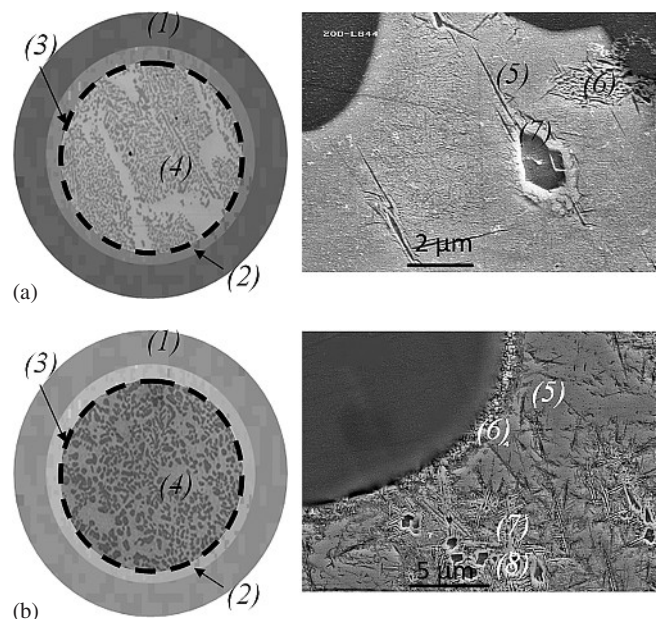


Fig. 9. Schematic drawing of the diffusion sequence and SEM picture after etching of the annealed sample (mass fraction of 0.2 Sn and 0.06 P) (a) at 917 K, and (b) at 915 K.

poses for both samples the three-phase region β - γ -Cu₃P for the detected concentrations in the centre of the samples. At first, it was not possible to detect γ in the micrographs and first SEM investigations, so etching was applied. The SEM pictures in Fig. 9 show the etched samples. The visible microstructure in Fig. 9b shows that β (5) seems to transform to a brighter needle-like structure (6, 7), especially at the boundary around Cu₃P (6). Here, it is visible that either a third phase, which could be γ according to the obtained Sn content, has been formed or a transition occurs appearing as a very fine, needle-like structure. The detected concentration in point (8), which is located in a dark, apparently deeper area than the surrounding, has a mass fraction of 0.20 Sn and no P. This could indicate that in this area α phase starts to form. In this case it could also be that the bright needles are forming δ . For sure it has to be kept in mind, that the concentrations of structures around and smaller than 1 μm cannot be measured properly due to the limitation of the resolution of the SEM measurements. In addition, the uneven surface caused by etching has a certain influence on the concentration measurement and with that this is just a first, rough interpretation.

Based on the fact, that these two samples do not show an indication for a liquid state during annealing, it is thought that the ternary point has to be situated above 915 K. ThermoCalc calculations (database CuSnII [22]) and Miettinen [6] propose the ternary eutectic point at around 917 K. Based on the observed phase distributions, this point can be confirmed to lie between 921 K and 915 K.

5. Conclusions

The presented study discusses the numerical description of the ternary phase diagram Cu–Sn–P in the Cu-rich corner based on calculations performed with the software ThermoCalc applying the database CuSnII [22] (mainly based on the assessment work of [6]) in comparison to experimental work based on annealing experiments combined with LM and SEM investigations.

The experimental observations show good agreement with the proposed ternary phase diagram of [6]. The detection of γ in the annealing experiment at 917 K and 919 K is in good agreement with the thermodynamic calculations but contrary to the absence of γ in the DTA measurements of [7]. Here further investigations are ongoing to gain more information about the appearance of the γ phase and to justify its presence. ε was not detected in the recent experimental work. This could be explained by the fact that, according to literature [4, 26, 27], ε is thought to form after very long diffusion times in the order of months or years and therefore it is not important for technical bronze alloys with Sn up to a mass fraction of 0.2.

The observed phase distribution, especially in the annealing sample at 921 K, indicates that the phase transition as proposed by [5] $L + \alpha \rightarrow \beta + \text{Cu}_3\text{P}$ should rather be an eutectic transition of $L \rightarrow \alpha + \beta + \text{Cu}_3\text{P}$ at approximately CuSn15P5. ThermoCalc (database CuSnII [22]) and Miettinen [6] propose this point at around 917 K. Based on the observed phase distributions, this point can be confirmed to lie between 921 K and 915 K.

This work is financially supported by the Austrian Christian-Doppler Research Society and Wieland Werke, Vöhringen for which the

authors kindly acknowledge. Besides we want to thank Prof. J. Ågren (KTH) for the scientific support and for the possibility of SEM investigations at the “Chair of Mineralogy and Petrology” of the University of Leoben.

References

- [1] J. Verö: *Z. anorg. allgem. Chemie* (1932) 257.
- [2] O. Bauer, M. Hansen: *Z. Metallkd.* (1930) 367.
- [3] R. Chadwick: *J. Inst. Met.* (1939) 331.
- [4] K. Dies: *Kupfer und Kupferlegierungen in der Technik*, Springer Verlag, Berlin (1967).
- [5] G. Effenberg, S. Ilyenko: *Landolt-Börnstein-Group IV* (2007) 355.
- [6] J. Miettinen: *Calphad* (2001) 67.
DOI:10.1016/S0364-5916(01)00031-1
- [7] T. Takemoto, I. Okamoto, J. Matusumura: *Trans JWRI* (1987) 73.
- [8] OF. Hudson, EF. Law: *J. Inst. Met.* (1910) 161.
- [9] L.C. Glaser, H.J. Seemann: *Z. Techn. Physik* (1926) 42.
- [10] L.C. Glaser, H.J. Seemann: *Z. Techn. Physik* (1926) 90.
- [11] M. Hamazumi: *J. Hpn. Inst. Met.* (1937) 165.
- [12] M.L. Levi-Malvano, F.S. Orofino: *Gazz. Chim. Ital.* (1911) 269.
- [13] J. Agren, F.H. Hayes, L. Höglund, U.R. Kattner, B. Legendre, R. Schmid-Fetzer: *Z. Metallkd.* (2002) 128.
- [14] U. Kattner, G. Erickson, P. Spencer, M. Schalin, R. Schmid-Fetzer, B. Sundman, B. Jansson, B. Lee, T. Chart, A. Costa e Silva: *CALPHAD* (2000) 55.
- [15] J. Agren: *Scripta Mater.* (2002) 893.
DOI:10.1016/S1359-6462(02)00083-0
- [16] A. Costa e Silva, J. Agren, M.T. Clavaguera-Mora, D. Djurovic, T. Gomez-Acebo, B.J. Lee, Z.K. Liu, P. Miodownik, H.J. Seifert: *Science Direct* (2007) 53.
- [17] B. Hallstedt, N. Dupin, M. Hillert, L. Höglund, H.L. Lukas: *Computer Coupling of Phase Diagrams and Thermochemistry* (2007) 28.
- [18] M. Hillert: *CALPHAD* (1997) 143.
DOI:10.1016/S0364-5916(97)00019-9
- [19] M. Hillert, L. Höglund: *Scripta Mater.* (2004) 1055.
DOI:10.1016/j.scriptamat.2003.12.026
- [20] H. Larsson, A. Engström: *Acta Mater.* (2006) 2431.
DOI:10.1016/j.actamat.2006.01.020
- [21] M. Grasser, F. Mayer, A. Ludwig: *TMS* (2009) 47.
- [22] ThermoCalc: “CuSnII Database” *Pers. Com.* (2005).
- [23] G. Panzl: Bachelor work, University of Leoben, Leoben (2008).
- [24] M. Gruber-Pretzler: Dissertation, University of Leoben, Leoben (2008).
- [25] T.B. Massalsky, J.L. Murray, L.H. Bennet, H. Baker: *Binary Alloy Phase Diagrams*, American Society for Metals, Ohio (1986).
- [26] H. Schumann: *Leipzig Dt. Verlag für Grundstoffind.*, Leipzig, (1990) 504.

(Received February 14, 2011; accepted April 12, 2012)

Bibliography

DOI 10.3139/146.110789
Int. J. Mat. Res. (formerly *Z. Metallkd.*)
 103 (2012) E; page 1–7
 © Carl Hanser Verlag GmbH & Co. KG
 ISSN 1862-5282

Correspondence address

DI Dr. mont. Monika Grasser
 Weizelsdorf 148
 A-9162 Strau, Austria
 Tel.: 0043 664 7300 9292
 E-mail: monika.grasser@htl-ferlach.at

You will find the article and additional material by entering the document number **MK110789** on our website at www.ijmr.de